[CANCER RESEARCH 64, 2212–2221, March 15, 2004]

Dysregulation of Sterol Response Element-Binding Proteins and Downstream Effectors in Prostate Cancer during Progression to Androgen Independence

Susan L. Ettinger, Richard Sobel, Tanis G. Whitmore, Majid Akbari, Dawn R. Bradley, Martin E. Gleave, and Colleen C. Nelson

The Prostate Centre at Vancouver General Hospital, Vancouver, British Columbia, Canada

ABSTRACT

Androgen ablation, the most common therapeutic treatment used for advanced prostate cancer, triggers the apoptotic regression of prostate tumors. However, remissions are temporary because surviving prostate cancer cells adapt to the androgen-deprived environment and form androgen-independent (AI) tumors. We hypothesize that adaptive responses of surviving tumor cells result from dysregulated gene expression of key cell survival pathways. Therefore, we examined temporal alterations to gene expression profiles in prostate cancer during progression to androgen independence at several time points using the LNCaP xenograft tumor model. Two key genes, sterol response element-binding protein (SREBP)-1 and -2 (SREBP-1a,-1c, and -2), were consistently dysregulated. These genes are known to coordinately control the expression of the groups of enzymes responsible for lipid and cholesterol synthesis. Northern blots revealed modest increased expression of SREBP-1a, -1c, and -2 after castration, and at androgen independence (day 21–28), the expression levels of both SREBP-1a and -1c were significantly greater than precastrate levels. Changes in SREBP-1 and -2 protein expression were observed by Western analysis. SREBP-1 68-kDa protein levels were maintained throughout progression, however, SREBP-2 68-kDa protein expression increased after castration and during progression (3-fold). SREBPs are transcriptional regulators of over 20 functionally related enzymes that coordinately control the metabolic pathways of lipogenesis and cholesterol synthesis, some of which were likewise dysregulated during progression to androgen independence. RNA levels of acyl-CoA-binding protein/diazepam-binding inhibitor and fatty acid synthase decreased significantly after castration, and then, during progression, increased to levels greater than or equal to precastrate levels. Expression of farnesyl diphosphate synthase did not decrease after castration but did increase significantly during progression to androgen independence. Levels of SREBP cleavage-activating protein, a regulator of SREBP transcriptional activity, decreased after castration and increased significantly at androgen independence. In clinical prostate cancer specimens from patients with varying grades of disease, the stained tissue sections showed high levels of SREBP-1 protein compared with noncancerous prostate tissue. After hormone withdrawal therapy, tumor levels of SREBP-1 decreased significantly after 6 weeks. AI tumors expressed significantly higher levels of SREBP-1. In summary, the LNCaP xenograft model of human prostate cancer as well as clinical specimens of prostate cancer demonstrated an up-regulation of SREBPs and their downstream effector genes during progression to androgen independence. As the AI phenotype emerges, enzymes critical for lipogenesis and cholesterol synthesis are activated and likely contribute significantly to cell survival of AI prostate cancer.

INTRODUCTION

Androgen ablation is the only form of systemic therapy demonstrated to prolong life in men with advanced prostate cancer. Removal of androgen induces apoptosis of prostate epithelial cells and regression of prostate tumors. Despite high initial response rates, remissions are temporary because surviving prostate cancer cells emerge with an androgen-independent (AI) phenotype. Thus, one of the main obstacles for curing advanced prostate cancer by androgen ablation is AI progression, a complex process involving dysregulated gene expression pathways that result in adaptive up-regulation of cell survival genes, ligand-independent androgen receptor transactivation, and activation of alternative growth factors or metabolic pathways (1).

Because prostate cancer varies in its biological aggressiveness, androgen sensitivity, and histological appearance, a single model that precisely mimics the diverse human condition does not exist. However, the LNCaP xenograft model does reflect many aspects of AI progression because it is androgen sensitive and prostate-specific antigen (PSA)-secreting (2, 3). As in human prostate cancer, serum PSA levels in this model are regulated by androgens and proportional to tumor volume in the intact animal (4). After castration, serum and tumor cell PSA levels decrease up to 80% and remain suppressed for 2–3 weeks. Beginning 3–4 weeks after castration, however, PSA production gradually increases above precastrate levels in the absence of testicular androgens, indicating the onset of AI PSA gene expression (5–7). AI progression in the LNCaP model is defined by the up-regulation of PSA in the absence of androgens. How PSA is re-expressed in androgen independence remains an intensive area of research focus. In general, it is hypothesized that escape from androgen-regulated PSA production may occur by either ligand-independent activation of the androgen receptor or up-regulation of alternative nonandrogenic pathways of signal transduction (5).

Characterization of the drift in gene expression caused by androgen ablation in the LNCaP tumor model mediating tumor progression to androgen independence provides insights into biological mechanisms and may facilitate the identification of prognostic indicators and therapeutic targets. We compared gene expression profiles at specified time points before and after castration in androgen-dependent, early postcastration, and AI recurrent LNCaP tumors to identify genes and gene clusters that become dysregulated during AI progression in the LNCaP tumor model. Several genes that are known to be androgen-regulated (including PSA) decreased after androgen withdrawal but were re-expressed during AI progression, indicating that perhaps all androgen receptor-regulated genes are up-regulated in androgen independence. Such androgen receptor-regulated genes include the sterol response element-binding protein (SREBP) family of transcriptional regulators that coordinately activate the expression of the cascades of genes associated with lipid and cholesterol synthesis as depicted in Fig. 1 (8). SREBP-1 and -2 protein isoforms (which share 45% homology) are derived from separate genes [SREBP-1a and -1c are splice variants (9, 10)]. SREBPs are transcription factors of the basic helix-loop-helix-Zip family and consist of approximately 1150 amino acids organized into three functional domains, an NH_2-terminal DNA-binding domain, a central transmembrane domain inserted into the endoplasmic reticulum, and a COOH-terminal regulatory domain (11). The NH_2 terminus and the COOH terminus are cytosolic and are anchored by two *trans*-membrane domains separated by a small loop that extends into the lumen of the endoplasmic reticulum and nuclear envelope (12, 13). The COOH terminus of SREBP interacts with the WD (tryptophan aspartic acid) repeat domain of SREBP cleavage-activating protein (SCAP) that is functionally regulated in part by

Received 8/1/02; revised 1/14/04; accepted 1/15/04.

Grant support: Grants from the National Cancer Institute of Canada.

The costs of publication of this article were defrayed in part by the payment of page charges. This article must therefore be hereby marked *advertisement* in accordance with 18 U.S.C. Section 1734 solely to indicate this fact.

Requests for reprints: Colleen C. Nelson, Prostate Cancer Research, Jack Bell Research Centre, 2660 Oak Street, Vancouver, British Columbia, Canada V6H 3Z6.

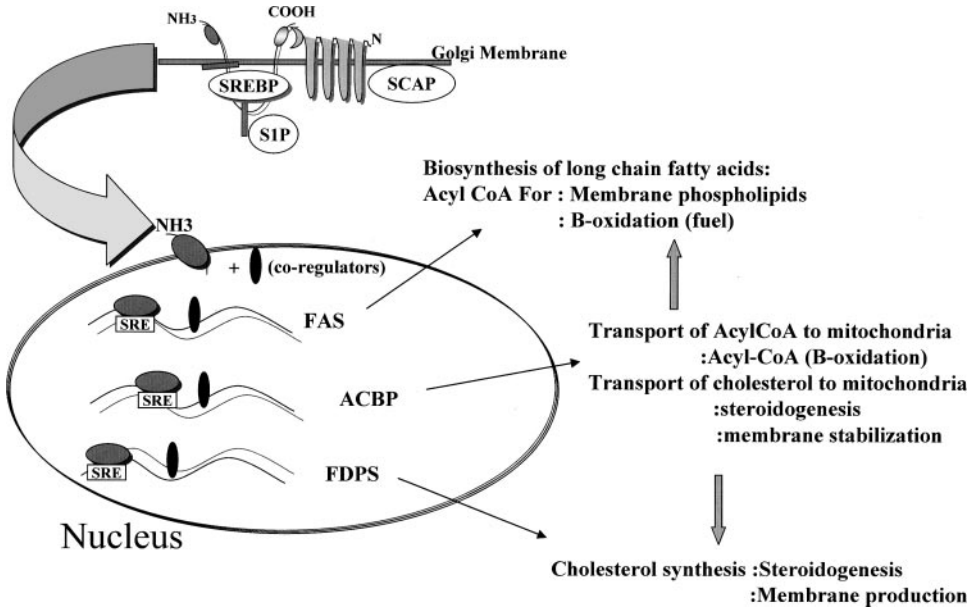

Fig. 1. The roles and regulation of sterol response element-binding proteins (SREBPs) in prostate cancer cells. SREBP cleavage-activating protein and SREBP, both normally regulated by androgens, become dysregulated during progression to androgen independence. After two cleavage events initiated by SREBP cleavage-activating protein/site-1-protease, the 68-kDa NH_3 domain of SREBP is transported into the nucleus, where it binds the sterol response element in the promoter of genes involved in fatty acid and cholesterol synthesis and transport [fatty acid synthase (*FAS*), acyl-CoA-binding protein (*ACBP*), and farnesyl diphosphate synthase (*FDPS*)]. Other coregulatory factors are also required for transcription of these genes. Fatty acid synthase enzyme generates long-chain fatty acids including acyl-CoA (a source of energy and membrane phospholipid). Acyl-CoA-binding protein/diazepam-binding inhibitor transports acyl-CoA to the mitochondria, where it undergoes β-oxidation to provide energy for the cell. It is also a component of mitochondrial membrane phospholipids. Farnesyl diphosphate synthase plays a role in cholesterol synthesis and membrane production. SREBP-1a and -1c transcriptionally regulate enzymes in both pathways, whereas SREBP-2 is thought to primarily regulate cholesterol synthesis (8).

sterol levels (14). The SREBP/SCAP complex is thought to move to the Golgi, where an enzyme, site-1-protease, cleaves SREBP between the lysine and serine residues of the RSVLS (arginine, serine, valine, leucine, and serine) domain within the lumen of the Golgi when sterols are limiting (15). This cleavage enables a second enzyme to cleave a site within the membrane, resulting in the release and translocation of a 68-kDa NH_2-terminal domain (basic helix-loop-helix) peptide to the nucleus, where it transactivates genes containing sterol-regulatory elements (16). Alternatively SREBP may be cleaved by caspase 3 to activate its nuclear translocation and subsequent transcriptional activation (17, 18). In the nucleus, SREBPs bind the sterol-regulatory element in the enhancer region of several genes encoding enzymes of cholesterol biosynthesis, unsaturated fatty acid biosynthesis, triglyceride biosynthesis, and lipid uptake [low-density lipoprotein (LDL) receptor; Ref. 19]. As part of a feedback mechanism, high cholesterol levels inhibit the SREBP/SCAP complex from recruiting or activating site-1-protease and therefore prevent release of the active basic helix-loop-helix fragment (20). SREBPs are androgen-regulated members of a pathway regulating cholesterol and acyl-CoA transport and fatty acid synthesis (8, 21) that are critical to cell proliferation and survival. We hypothesize that dysregulated expression of SREBPs after castration may help mediate AI progression through the downstream pathways regulated by SREBPs that ensure maintenance of cholesterol and fatty acid synthesis.

This report provides the first demonstration in an *in vivo* prostate cancer tumor model that expression of SREBPs as well as some of their downstream effectors [acyl-CoA-binding protein/diazepam-binding inhibitor (ACBP/DBI), fatty acid synthase (FAS), and farnesyl diphosphate synthase (FDPS)] becomes dysregulated during progression to androgen independence. Additionally, the expression of a posttranslational regulator of SREBPs, SCAP, was increased during progression. Western analysis and immunohistochemistry demonstrated that SREBP-1 (68 kDa) protein level was maintained in LNCaP tumors after castration and during progression to androgen independence. SREBP-2 (68 kDa) protein expression increased significantly after castration and during progression. Interestingly, staining of human prostate tumors showed elevated levels of SREBP-1 protein compared with normal prostate tissue. Androgen ablation by neoadjuvant hormone therapy before radical prostatectomy resulted in decreased protein levels of SREBP-1; however, after several months, when tumors progressed to androgen independence, SREBP-1 protein levels once again increased. These results provide the first *in vivo* demonstration in both xenograft tumors and clinical specimens of human prostate cancer of the dysregulation of SREBPs and their downstream effector gene targets during progression to androgen independence.

MATERIALS AND METHODS

***In Vitro* Model: Cell Culture.** Cultured LNCaP cells (derived from the lymph node metastasis of a prostate cancer patient), passage 35–45, were maintained in RPMI 1640 with 5% FCS and antibiotic/antimycotic at 37°C and 5% CO_2 (22).

***In Vivo* Model: LNCaP Tumor Progression to Androgen Independence.** LNCaP cells (2×10^6) were grown *in vitro* as described above, trypsinized, pelleted, and coinoculated with 120 μl of Matrigel (50:50 volume ratio of cells to Matrigel; Becton Dickinson Labware). Cells were equally distributed at six sites by s.c. injection (right and left shoulder, right and left flank, and right and left hip) in 6–8-week-old athymic nude mice (BALB/c strain; Charles River Laboratory) or severe combined immunodeficient mice under methoxyfluorane anesthesia. Mice were housed in a barrier unit and monitored every 3–5 days for PSA levels and tumor growth.

Serum PSA Levels. Blood samples were collected by tail vein incision, and the serum was stored at –20°C until assayed for PSA. Serum PSA was determined using an enzymatic immunoassay kit (Abbott IMX) according to the manufacturer's protocol. Time to AI PSA expression was defined as the duration of time required after castration for serum PSA levels to return to or increase above precastrate levels.

Tumor Harvest. When tumor size reached approximately 1.5 cm in diameter (6–8 weeks after injection), and the serum PSA was >100 ng/ml, two

animals were sacrificed by carbon dioxide asphyxiation, and the tumors were resected. The tumor was further dissected, and segments were either placed in TRIzol (Invitrogen, Carlsbad, CA) and frozen immediately at −80°C or placed in formalin or liquid nitrogen. The remaining animals were surgically castrated under methoxyfluorane anesthesia and monitored for PSA levels for up to 5 weeks. Tumors were harvested at several points along the PSA curve. The epithelial:stromal ratio is consistent within this tumor model and varies <10% between tumors, as assessed by immunohistochemistry of cytokeratin 14 (epithelium) and vimentin [stroma (2)].

Northern Analysis. Total RNA (15 μg) isolated in TRIzol (prepared according to the manufacturer's protocol) was denatured in deionized formaldehyde/formamide/3-(*N*-morpholino)propanesulfonic acid (Fisher Biotech) sample buffer and subjected to electrophoresis through a denaturing 1% agarose, 3-(*N*-morpholino)propanesulfonic acid, and deionized formaldehyde gel at 75 V for 2 h in 1× 3-(*N*-morpholino)propanesulfonic acid buffer. The RNA was transferred to a nylon membrane (Biodyne B; Pall Gelman Laboratory, East Hills, NY) overnight in 20× SSC (pH 7.0). The RNA was UV cross-linked to the membrane (UV Stratalinker 1800; Stratagene) according to the manufacturer's instructions. The membrane was hydrated with diethyl pyrocarbonate-treated water and then prehybridized in Expresshyb (Clontech) and denatured salmon testis DNA (100 μg/ml) at 65°C for 1 h in a hybridization oven (Stack and Shake ThermoHybaid, Ashford, Middlesex, United Kingdom).

Human cDNA probes were generated by reverse transcription of total RNA from LNCaP cells using Superscript II (Life Technologies, Inc.) and random hexamers [$p(dN)_6$, Roche] as primers. The cDNA generated was used as a template for PCR with the following primer pairs from Operon: 18S RNA, 5′-aaacggctaccacatccaag-3′ (sense) and 5′-cctccaatggatcctcgtta-3′ (antisense); SREBP-1a, 5′-tcagcgaggcggctttggagcag-3 (sense) and 5′-catgtcttcgatgtcggtcag-3′ (23); SREBP-1c, 5′-ggaggggtagggccaacggcct-3′ (sense) and 5′-catgtcttcgaaagtgcaatcc-3′ (23); ACBP/DBI, 5′-ctgcagaggaggttaggcac-3′ (sense) and 5′-tggcacagtaaccaaatcca-3′ (antisense). PCR products were cloned into pCRII-TOPO (Invitrogen, Life Technologies, Inc.), and then the resulting construct was transformed into chemically competent *Escherichia coli* according to the manufacturer's instructions. A ~2.5-kb DNA for SCAP and a 1.9-kb DNA for FDPS were obtained from a sequence-verified library of clones from Research Genetics by PCR of plasmid DNA using the BmapF (5′-ctgcaaggcgattaagttgggtaac-3′) and BmapR (5′-gtgagcggataacaattttcacacaggaaacagc-3′) primers with an annealing temperature of 60°C and an extension time of 1 min. Two 457-kb probe DNAs for SREBP-2 and a 420-kb DNA for FAS were generated from plasmids by PCR (pSREBP-2, ATCC 79816; pFAS, ATCC 78751). The primers were BP-2F1 (5′-actctgcaagtcaaggtttc-3′) and BP2-R2 (5′-ggctgccatctgtcttcagt-3′) for the SREBP-2 probe 1 and BP2-F2 (5′-gcctcagatcatcaagacag-3′) and BP2-R1 (5′-ccagctcagcaccatgttc-3′) for SREBP-2 probe 2. Primers for the FAS probe were FAS-F (5′-gaggtggtgattgccggcatg) and FAS-R (5′-gttggccatcatcgctcgct-3′). All probes were gel-purified, sequence-verified (ABI Prism; PE Biossystems, Mississauga, Canada), and quantitated. Probes were radiolabeled using random hexamers according to an oligolabeling kit (Pharmacia) to a specific activity of $1–2 \times 10^9$ dpm/μg and then hybridized to the membranes overnight at 65°C. Membranes underwent high-stringency washes at 65°C and were exposed to Kodak film and a phosphorimager screen (Fuji) and quantitated on a Typhoon 9410 PhosphorImager (Molecular Dynamics) using Imaquant software. Ribosomal 18S RNA was used as a loading control, and all phosphorimages were normalized to 18S RNA before statistical analyses were performed [one-way ANOVA with Student-Newman-Keuls Method (SigmaStat Statistical Software Version 2; SPSS Inc.)].

Western Analysis. Tumor tissue was homogenized in radioimmunoprecipitation assay buffer [PBS, 1% Igepal (Sigma), 0.5% deoxycholate, 0.1% SDS, protease inhibitor mixture (Roche)], and protein concentrations were assessed by the BCA method (Pierce, Rockford, IL). Equivalent concentrations of protein (10 μg), mixed with SDS sample buffer containing DTT, were boiled at 90°C for 3 min before loading on 10% polyacrylamide gels. Proteins were transferred electrophoretically onto polyvinylidene difluoride (Millipore, Bedford, MA) using a wet transfer apparatus (Bio-Rad, Hercules, CA). Blots preincubated with Tris buffer [20 mM Tris, 146 mM NaCl (pH 7.4)] and 5% skim milk were blotted with monoclonal antibodies (1:1,000) to either SREBP-1 (clone 2A4; NeoMarkers, Medicore) or SREBP2 (clone 1C6; NeoMarkers, Medicore), overnight at 4°C. We confirmed our results with a SREBP-1 antibody kindly donated by Drs. M. S. Brown and J. L. Goldstein. After incubation with the secondary antibody (1:10,000) and several washes, blots were soaked in enhanced chemiluminescence reagents (Amersham Pharmacia, Baie d'Urfe, Quebec, Canada) and exposed to Kodak Biomax MR film (Eastman Kodak, Rochester, NY) for 30 s to 1 min. Bands were quantitated on a Bio-Rad Gel Doc 2000 system. Protein expression levels were normalized to tubulin before statistical analyses were performed ($n = 3$; Student's paired t test).

Tissue Microarray Slide Preparation. For human prostate cancer Gleason grade arrays, a total of 400 tumors were arrayed: 34 benign tumors; 70 Gleason grade 2 tumors; 235 Gleason grade 3 tumors; 34 Gleason grade 4 tumors; and 27 Gleason grade 5 tumors. The human prostate cancer tissue array comprised 150 specimens (2 samples/tumor specimen) from either patients who had not received hormone therapy or patients who had received neoadjuvant hormone therapy for 3, 6, or 8 months before radical prostatectomy. Tumors that had acquired AI growth were also included. AI status of the AI clinical specimens was based on biochemical progression in which patients had rising PSA values despite castrate levels of testosterone while undergoing androgen ablation therapy and clinical progression including local bladder outlet obstruction and/or bone scan progression. Sections (5 μm) were cut with a microtome by use of an adhesive-coated tape sectioning system (Instrumedics, Hackensack, NJ) to support the adhesion of the array elements.

Immunohistochemistry. Mounted tissue was rehydrated, and endogenous peroxidase activity was blocked with methanol:30% H_2O_2 (9:1). Antigen retrieval was enhanced using commercial antigen unmasking solution (Dako Target Retrieval Solution; Dako Corp., Carpinteria, CA) with the autoclave method. BSA was applied for 1 h at 25°C to block the nonspecific binding sites on the slides, which were then incubated in a humidified chamber overnight at 4°C with a 1:100 dilution of SREBP-1 antibody (commercial antibodies tested did not detect SREBP-2 by immunohistochemistry). After primary incubation, tissue was washed three times with PBS and incubated with a goat antirabbit horseradish peroxidase-conjugated IgG secondary antibody (Upstate Biotechnology, Lake Placid, NY) used at a 1:400 dilution for 30 min at 25°C. The antigen was visualized by a subsequent 5-min incubation with diaminobenzidine tetrahydrochloride before counterstaining with hematoxylin. Tissues were covered with mounting media (Permount; Fisher Scientific, Fair Lawn, NJ) and a coverslip.

Negative control slides were processed in an identical fashion to those described above, with the substitution of normal goat nonimmune serum for the primary antiserum. No color reactions were observed in negative control slides. Photomicrographs were taken through a Leica DMLS microscope coupled to a digital camera (Photometrics CoolSNAP; Roper Scientific, Inc., Glenwood, IL) and the corresponding computer software.

Scoring of SREBP-1 Staining. The staining intensity of SREBP-1 was evaluated and scored as follows: specimens were graded from 0 to +4 intensity, representing the range from no staining to intense staining. All comparisons of staining intensity and percentages were made at ×400 magnification. Simultaneously expression of SREBP-1 protein was recorded as nuclear, cytoplasmic, and both. The percentage of stained area (combination of intensity and surface area) was measured by Image Plus software (Media Cybernetics) and assessed by the pathologist (M. A.). ANOVA was performed.

RESULTS

To examine changes in gene expression during prostate cancer progression to androgen independence, LNCaP tumors were harvested at various times before and after castration throughout the progression time series. RNA was initially analyzed using cDNA microarrays to derive gene expression profiles. Alteration to the expression levels of key transcription factors was studied in greater depth to determine potential cascades of gene activation that may functionally impact prostate cancer progression to androgen independence. Of particular interest was the observation that SREBPs appeared to be up-regulated during prostate cancer progression in the LNCaP tumor model. SREBPs are transcription factors that are known to coordinately regulate genes involved in two major pathways including enzymes of fatty acid synthesis as well enzymes of cholesterol synthesis and transport as depicted in Fig. 1 (8).

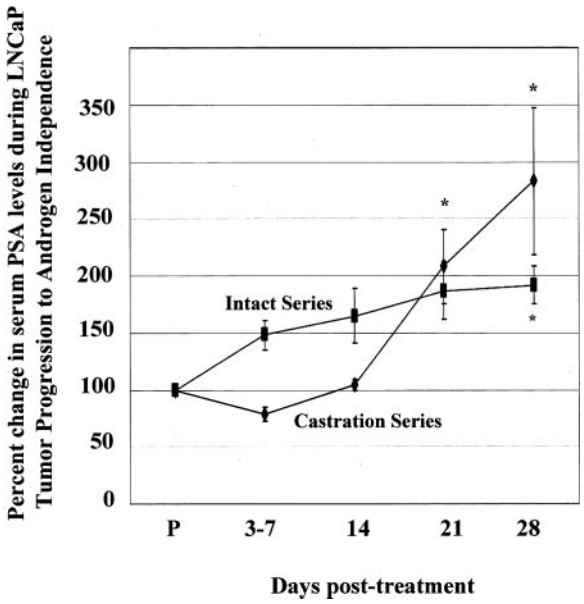

Fig. 2. Serum prostate-specific antigen levels decrease after castration and then undergo a rapid rate of increase during prostate tumor progression to androgen independence. Prostate-specific antigen levels in the castration series and intact series are expressed as a percentage change (mean ± SE) from precastrate (*P*) in LNCaP tumor model assessed at 3–28 days postcastration. ∗, statistical significance ($P < 0.05$).

Serum PSA Levels Change during Tumor Progression to Androgen Independence. Serum PSA levels were decreased 3–7 days after castration (Fig. 2). After 21–28 days, serum PSA levels increased significantly ($P < 0.05$), indicating an AI phenotype. The PSA level of intact hosts increased at a continuous rate for 21 days and then reached a plateau by 28 days.

SREBP-1 and SREBP-2 mRNA and Protein Expression Were Altered during Progression to Androgen Independence. To verify the array-based observations, we performed Northern blot analysis on total RNA isolated from several LNCaP tumor series with probes specific for SREBP-1a, -1c, and -2. These results demonstrated that SREBP-1a, -1c, and -2 were up-regulated during progression. RNA expression of SREBP-1a and -1c, at androgen independence (day 28 postcastration), was significantly increased compared with expression in tumors from intact mice (Fig. 3, *A*−*D*). The elevated expression of these transcription factors was modest but significant in six separate tumor progression series ($P < 0.05$).

The expression of SREBP-2 was also moderately increased after 21–28 days, compared with the levels determined in tumors from intact mice (Fig. 3, *E* and *F*); however, these differences were not significant. Generally, expression of SREBPs displayed trends to increased levels at androgen independence that paralleled significant trends found in downstream effectors as documented below.

SREBP-1 and -2 Protein Expression Was Altered during Progression to Androgen Independence. Western analysis of SREBP-1 revealed that the uncleaved 125-kDa product changed with progression. Levels were decreased at 3–7 days and reached a nadir at 14 days. By 21–28 days, protein expression increased compared with day 14, but not significantly, and did not reach precastrate levels (Fig. 4, *A* and *B*). Expression levels of the cleaved form of SREBP-1 (68 kDa) changed slightly during progression (Fig. 4, *A* and *B*). The increased levels of cleaved protein at day 14 correlated with decreased levels of full-length protein at this time. The antibody does not distinguish between SREBP-1a and -1c isoforms; therefore, we cannot determine their specific expression profiles or determine correlation between mRNA and protein. Unlike SREBP-1, SREBP-2 protein expression of the cleaved form (68 kDa) increased significantly during progression to levels 350% above precastrate levels ($P < 0.05$; Fig. 4, *C* and *D*).

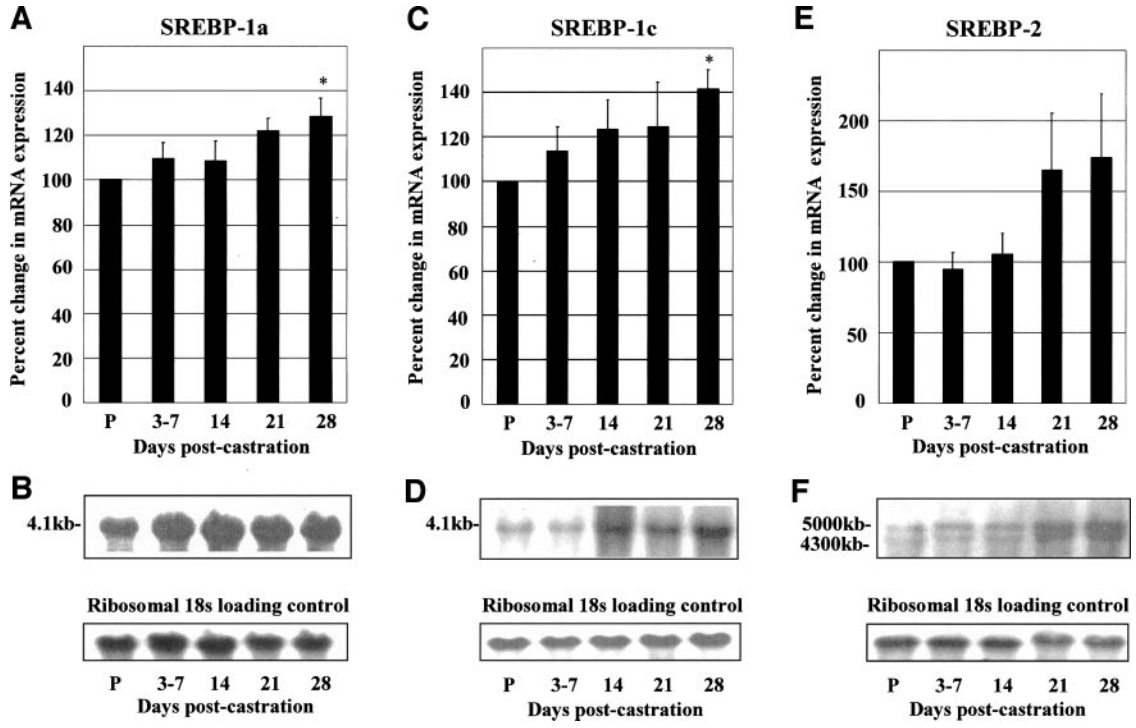

Fig. 3. Sterol response element-binding protein (SREBP)-1a, -1c, and -2 are transcriptionally regulated during prostate progression to androgen independence. Expression of SREBP-1a (*A*), SREBP-1c (*C*), and SREBP-2 (*E*) mRNA as a percentage change (mean ± SE) from precastrate (*P*) in LNCaP tumors was assessed after postcastration intervals of 3–7, 14, 21, and 28 days by Northern analysis, quantified by phosphorimaging ($n = 6$ for each time point), and normalized to 18S RNA expression. Representative Northern blots of SREBP-1a (*B*), -1c (*D*), and -2 (*F*) and ribosomal 18S RNA expression in LNCaP tumors harvested during progression (precastrate to 28 days postcastration) are shown. ∗, statistical significance ($P < 0.05$).

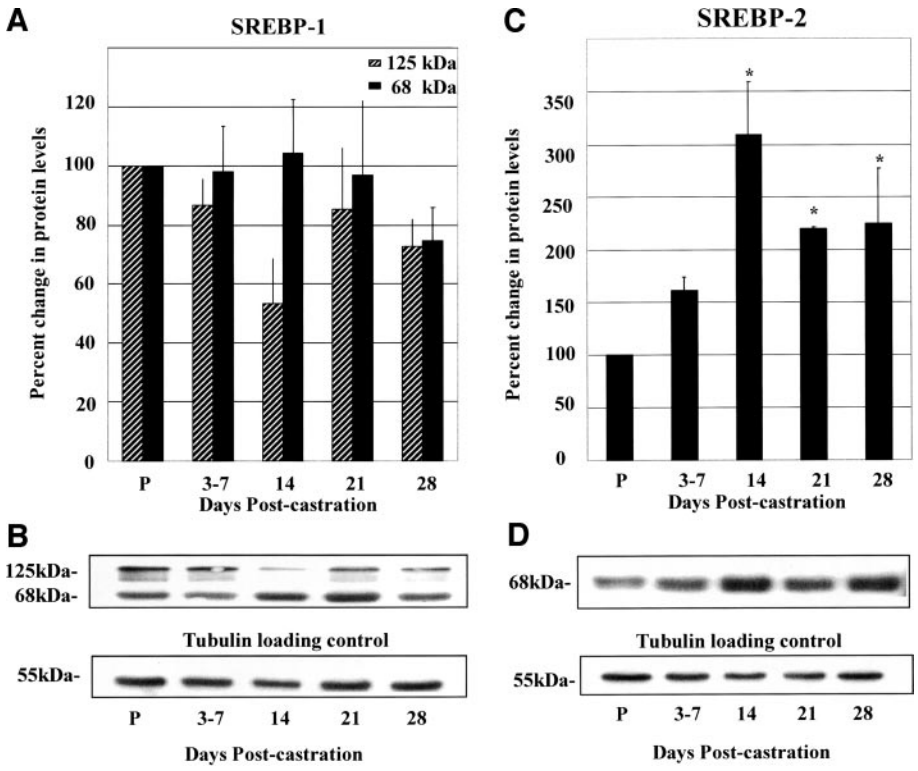

Fig. 4. Sterol response element-binding protein (SREBP)-1 and -2 protein expression changes during progression to androgen independence. Western analysis of full-length (125-kDa) and cleaved (68-kDa) SREBP-1 (*A*) and -2 (*C*) expressed as a percentage change (mean ± SE) from precastrate (*P*) in LNCaP tumors assessed after postcastration intervals of 3–28 days during progression ($n = 3$ for each time point) is shown. A representative tumor progression series at precastrate (*P*) and 3–28 days postcastrate intervals is shown. The 125-kDa proform and the 68-kDa active form of SREBP-1 (*B*) and -2 (*D*) are indicated. Protein (10 μg; from tissue homogenates), mixed with SDS sample buffer, was separated on 10% polyacrylamide gels and transferred electrophoretically onto nylon membrane. Tubulin was used as a loading control. ∗, statistical significance ($P \leq 0.05$).

Despite modest changes in SREBP-2 mRNA expression after castration, there were significant increases in 68-kDa protein levels during progression. These changes in 68-kDa SREBP-2 were greater than those documented for 68-kDa SREBP-1. We have been unable to obtain a specific antibody for mature (125-kDa) SREBP-2 that detects protein on Western blots, so we are unsure of the kinetics of cleavage events during progression. We have shown that throughout progression, levels of both 68-kDa cleavage products of SREBP-1 and -2 are present to interact with sterol response elements. Because SREBPs are regulated in part by the androgen receptor in prostate cancer cells, perhaps the reactivation of SREBPs at androgen independence occurs through a similar process, as does PSA expression in androgen independence.

To determine whether the up-regulation of SREBPs during progression functionally impacted the expression of genes known to be regulated by SREBPs, we examined the expression of key genes within the cascades of lipogenesis and cholesterol synthesis and acyl-CoA transport (ACBP, FAS, and FDPS; Fig. 1).

ACBP/DBI Expression Was Altered during Progression to Androgen Independence. It is known that ACBP/DBI is regulated in part indirectly by androgens in prostate cancer cells through the direct up-regulation of SREBP-1a mRNA (24). It is unclear whether other SREBP isoforms are equally effective in regulating ACBP/DBI expression. ACBP/DBI functions as a transporter of acyl-CoA and cholesterol into the mitochondria and thus plays a role in cholesterol-based biosynthesis. The profile of ACBP/DBI mRNA expression during progression correlated somewhat with the expression pattern seen for PSA, another androgen-regulated gene. After castration, ACBP/DBI mRNA expression was significantly decreased after 3–14 days compared with precastrate controls ($P < 0.05$). Levels returned to normal after 21–28 days ($P < 0.05$; Fig. 5, *A* and *B*), when androgen independence was reached. This may indicate a response to increased SREBPs at this time. Specific levels of SREBP-1a and -1c protein could not be measured; therefore, it was unclear which isoform was involved in the regulation of ACBP/DBI during progression to androgen independence.

FAS Expression Is Increased at Androgen Independence. As shown in Fig. 1, SREBPs coordinately regulate transcription of several enzymes involved in the biosynthesis of cholesterol and fatty acids. FAS is a key enzyme in the fatty acid synthesis cascade and has been shown to be regulated by SREBP-1a (21). Expression of FAS decreased after a 14-day period following castration and by 21 days had increased to levels greater than that found in tumors from intact mice ($P < 0.05$; Fig. 5, *C* and *D*). The levels continued to increase significantly during the 28-day follow-up. The kinetics of increased expression were similar to those of SREBP-1a and -1c (days 21–28), inferring a coordinated regulation during tumor progression to androgen independence of this pathway of genes involved in fatty acid synthesis.

FDPS Expression Increased during Progression to Androgen Independence. A downstream target of SREBPs involved in the cholesterol synthesis cascade, shown in Fig. 1, is FDPS, which is critical for metabolism and membrane production (8, 21). Expression levels of FDPS did not decrease significantly after castration but did increase gradually and, by 21–28 days, had increased to levels that were greater than those in tumors of intact mice (Fig. 5, *E* and *F*). The levels at 28 days were significantly elevated ($P < 0.05$). The profile of FDPS mRNA expression was similar to that of SREBP-2 (mRNA and protein) in that both were increased at androgen independence.

SCAP Expression Was Dysregulated during Tumor Progression. The observed increases in levels of downstream targets were greater than changes in levels of SREBPs. It was shown that in addition to up-regulation of SREBPs at the transcriptional level, the activation of SREBP protein was also being stimulated. Therefore, we examined the expression of a protein activator of SREBP function, the SREBP cleavage-activating protein (SCAP), to determine whether it was also aberrantly expressed during progression to androgen independence.

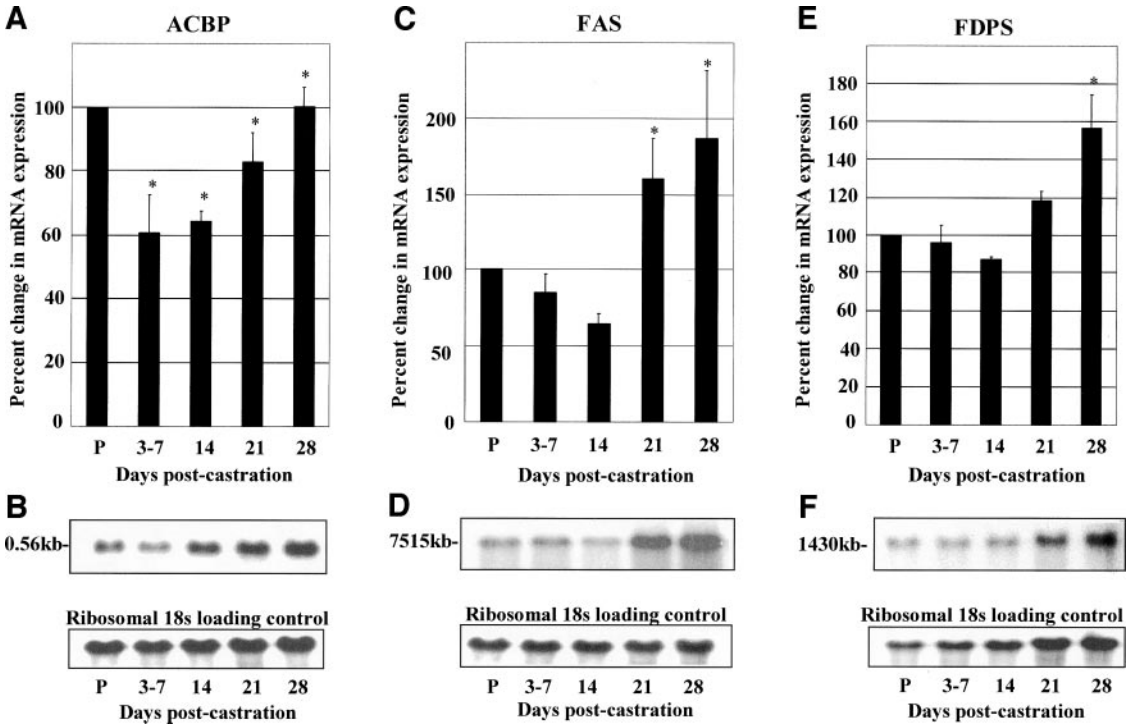

Fig. 5. Acyl-CoA-binding protein/diazepam-binding inhibitor (ACBP/DBI), fatty acid synthase (FAS), and farnesyl diphosphate synthase (FDPS) expression increases during prostate cancer progression to androgen independence. ACBP/DBI (*A*), FAS (*C*), and FDPS (*E*) mRNA expression as a percentage change (mean ± SE) from precastrate (*P*) expression in LNCaP tumors was assessed after postcastration intervals of 3–7, 14, 21, and 28 days by Northern analysis and quantified by phosphorimaging ($n = 4$ for each time point). Representative blots of ACBP/DBI (*B*), FAS (*D*), and FDPS (*F*) and ribosomal 18S RNA expression in LNCaP tumors harvested during progression (precastrate to 28 days postcastration) are shown. ∗, statistical significance ($P < 0.05$).

By Northern analysis, SCAP expression was significantly decreased 14 days after castration ($P < 0.05$) and significantly upregulated by 21 days and 28 days ($P < 0.05$; Fig. 6, *A* and *B*). The increased expression at 21 and 28 days correlated with significant increases in mRNA SREBPs at androgen independence. Expression of both SREBP and SCAP has been shown to be androgen regulated (23). Interestingly, the mRNA expression profile of SCAP closely mimics the expression profile of ACBP/DBI and FAS, downstream effectors of SREBPs. The lowest level of expression of ACBP/DBI, FAS, and SCAP occurred at day 14, followed by significant increases at 21–28 days. SCAP may play an important role in augmenting SREBP activity in tumor progression to androgen independence, but it may not be the only mechanism regulating SREBP function.

SREBP-1 Protein Expression Is Altered in Human Prostate Cancer Specimens. To determine whether SREBP expression is altered in clinical prostate cancer, a human prostate cancer tissue array comprised specimens from four types of prostatic tissue: (*a*) benign prostatic hypertrophy; (*b*) tumors from patients who had not received hormonal therapy; (*c*) tumors from patients who had received neoadjuvant hormonal therapy for 3, 6, or 8 months; and (*d*) tumors that had become AI. Tissue specimens were stained for SREBP-1. As can be seen in Fig. 7*A*, sections of benign prostatic hypertrophy showed a low level of staining for SREBP-1, compared with sections of untreated prostate cancer, which showed intense staining (Fig. 7*B*). After 6 weeks to 3 months of neoadjuvant hormonal therapy (Fig. 7, *C* and *D*), the prostate sections showed very little SREBP-1 staining. However, by 8 months of neoadjuvant hormonal therapy (Fig. 7*E*), levels of SREBP-1 had increased, and when tumors had reached androgen independence (Fig. 7*F*), the staining was very intense. Morphological changes related to androgen withdrawal therapy precluded assessing an exact Gleason grade, but in Fig. 7, the sections were all equivalent to Gleason grade 3. As seen in Fig. 7*G*, neoadjuvant hormone therapy administered for 6 weeks to 8 months significantly decreased the amount of SREBP-1 present in patient tumor samples ($P < 0.001$), but at androgen independence, SREBP-1 increased to levels seen without androgen ablation treatment.

DISCUSSION

Through array-based analysis, we have identified genes in the LNCaP tumor model that become dysregulated after castration and during progression to androgen independence. Data presented here characterize the cascades of genes coordinately regulated by the SREBPs, SREBP-1a, -1c, and SREBP-2, including ACBP/DBI, FDPS, FAS, and a posttranslational regulator of SREBP activity, SCAP, all of which are components of a pathway critical to survival. Tumor cells are highly metabolically active and proliferative; thus they require increased energy metabolism (citrate cycle) and membrane production (fatty acid and cholesterol synthesis). The proteins regulating fatty acid biosynthesis and cholesterol levels in prostate cells are regulated by androgens, including SREBPs (8, 21). SREBPs in turn regulate ACBP/DBI (24–26), FDPS, and FAS (8, 11, 21, 23, 27, 28). Recently, SCAP was shown to be regulated by androgens in prostate cells (23).

Androgens stimulated the expression of SREBP transcripts and precursor proteins in LNCaP cells *in vitro* and increased the nuclear content of the active 68-kDa fragment of SREBP (8, 11). Expression of SREBP-1a and -1c mRNA in our *in vivo* tumor progression series increased significantly when tumors reached androgen independence. There was a trend of increased expression of SREBP-2 mRNA during AI progression that did not quite reach significance. Protein expression of the uncleaved SREBP-1 125-kDa product was decreased at 14 days compared with precastrate levels but increased after 21–28 days. Interestingly, the cleaved 68-kDa product remained relatively con-

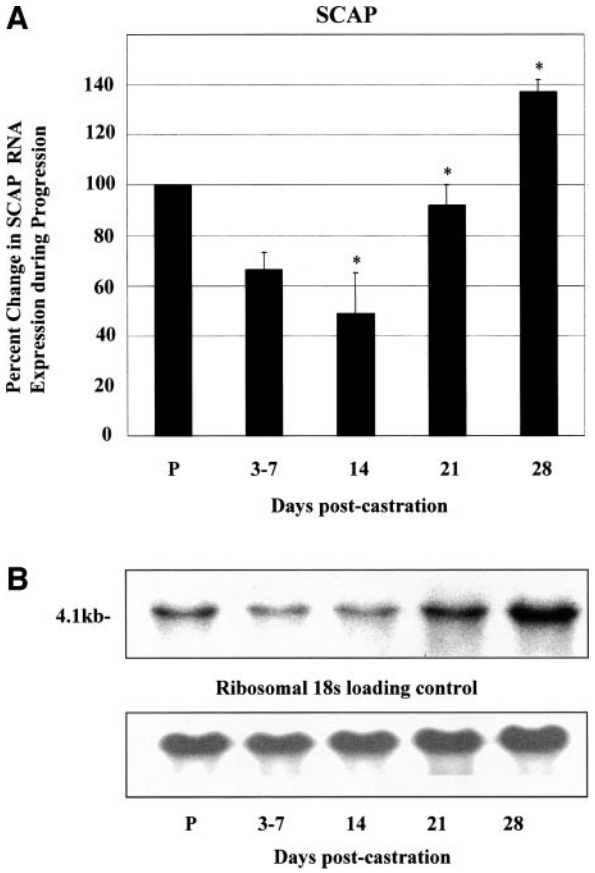

Fig. 6. Expression of a posttranslational activator of sterol response element-binding protein, sterol response element-binding protein cleavage-activating protein (SCAP), increases in progression to androgen independence. SCAP RNA expression (*A*) as a percentage change (mean ± SE) from precastrate (*P*) expression in LNCaP tumors was assessed at postcastration intervals of 3–7, 14, 21, and 28 days by Northern analysis and quantified by phosphorimaging ($n = 4$ for each time point). Representative blots of SCAP (*B*) and ribosomal 18S RNA expression in LNCaP tumors harvested during progression (precastrate to 28 days postcastration) are shown. *, statistical significance ($P < 0.05$).

stant, except for an increase at day 14 that coincided with the decrease in the 125-kDa product at this time, perhaps due to a cleavage event and/or accumulation as described below. SREBP-2 protein expression of the mature form (68 kDa) increased significantly after castration and remained elevated during progression. Mature forms of both SREBP-1 and -2 were present to activate transcription of downstream effectors (ACBP/DBI, FAS, and FDPS) at androgen independence. However, in the early postcastration period, despite the presence of SREBP transcription factors, SCAP, FAS, and ACBP/DBI mRNA expression decreased. It is possible that SREBP transcriptional activation of ACBP/DBI and FAS was modulated not just by SCAP but by signaling pathways and other factors/coregulators. Decreased SREBP activity during the early postcastration period may be due to several factors. Posttranslational modifications may play a role because it has been shown *in vitro* that phosphorylation of SREBP-1a at serine 117 by extracellular signal-regulated kinase 1/2 is necessary for its transcriptional activation of LDL receptor (29). In addition, SREBPs are weak activators of transcription and function more efficiently when activated by coregulatory transcription factors such as nuclear factor Y or Sp-1 (30). FAS expression, for instance, is also strongly influenced by coregulatory factors nuclear factor Y and Sp-1, whereas expression of ACBP and FDPS requires nuclear factor Y (30). Transcriptional repressors may also play a role in decreased SREBP activity. It has been reported that the Yin Yang-1 transcription factor, which is capable of negative and positive regulation, displaces nuclear factor Y, binds SREPB-1a, and disrupts binding to sterol response elements and thus may play a regulatory role in the transcription of some SREBP-responsive genes (31). Recent studies have shown that inhibition of the transcriptional activity of SREBP prevents its degradation, resulting in accumulation of SREBP proteins (32). This lack of degradation may account for the presence of mature SREBP proteins detected in our studies during the early postcastration period, when mRNA levels of SCAP, ACBP/DBI, and FAS were low.

In summary, in our *in vivo* model of prostate cancer, SCAP, SREBPs, and downstream effectors ACBP/DBI, FAS, and FDPS were all significantly elevated compared with intact controls when androgen independence was reached. The magnitude of expression and the temporal changes in expression of SREBPs differed from that seen in downstream effector genes during the early postcastration interval, indicating that several pathways were likely involved during this time to regulate the expression of these androgen-regulated genes.

Specific regulation of SREBP-1 and -2 appears to occur by different mechanisms during progression. Defining which isoform regulated specific genes was beyond the scope of this work; however, there appear to be several mechanisms to regulate transcription and processing of SREBPs including androgen levels, sterols, fatty acids, coregulators, and insig-1 and -2 (33). Differential regulation of SREBP-1 and -2 was reported by others previously. Together, these data suggest that, in general, SREBP-2 appears to be the main isoform that transcriptionally regulates the cholesterol biosynthesis genes and the LDL receptor, whereas SREBP-1a and -1c are transcriptional activators of fatty acid synthesis [in addition to cholesterol synthesis (28, 34)].

ACBP/DBI expression is regulated indirectly by androgen through the up-regulation and activation of SREBPs (24). ACBP/DBI is a multifunctional, highly conserved 10-kDa protein expressed in various tissues including rat brain and pancreas, bovine liver, Leydig cells, and glial cells as well as in yeast and bacteria (25). In our studies, LNCaP tumor ACBP/DBI levels decreased within a week of castration but then increased significantly over the next several weeks. Whereas the function of ACBP/DBI in tumors during progression to androgen independence is unknown, several potential roles may include supporting energy metabolism, steroidogenesis, membrane production, and transcription. ACBP/DBI binds with high affinity to cellular acyl-CoA (35, 36) and transports acyl-CoA to the mitochondria (37). Once inside the mitochondria, acyl-CoA undergoes B-oxidation to acetyl-CoA, which then generates ATP during the citric acid cycle and respiratory chain (37). ACBP/DBI may also play a role in steroid production because it transports cholesterol to the inner mitochondrial membrane, where it is loaded onto cholesterol side chain cleavage cytochrome-P450, initiating steroidogenesis (38–40).

Also within the mitochondria, ACBP/DBI has been shown to transport cholesterol to the peripheral benzodiazepine receptor, which is part of a heteromeric complex involved in the formation of a mitochondrial permeability transition pore (20). The peripheral benzodiazepine receptor/ACBP complex may play a role in preventing apoptosis by stabilizing the mitochondrial membrane by ensuring an adequate supply of cholesterol (41–43). Interestingly, a correlation of breast cancer cell aggressive phenotype with peripheral benzodiazepine receptor expression in the nuclear membrane has been documented (44). Peripheral benzodiazepine receptor in aggressive breast tumor cells regulated cell proliferation and cholesterol transport into the nucleus; however, the role of nuclear cholesterol is unknown. Nuclear ACBP/DBI is known to interact with the nuclear binding protein HNF-4a and thus may play a role in regulating transcription of genes involved in glucose and lipid metabolism (45).

Androgen enhances the expression of several lipogenic enzymes including those in the fatty acid synthesis pathway (FAS) and the

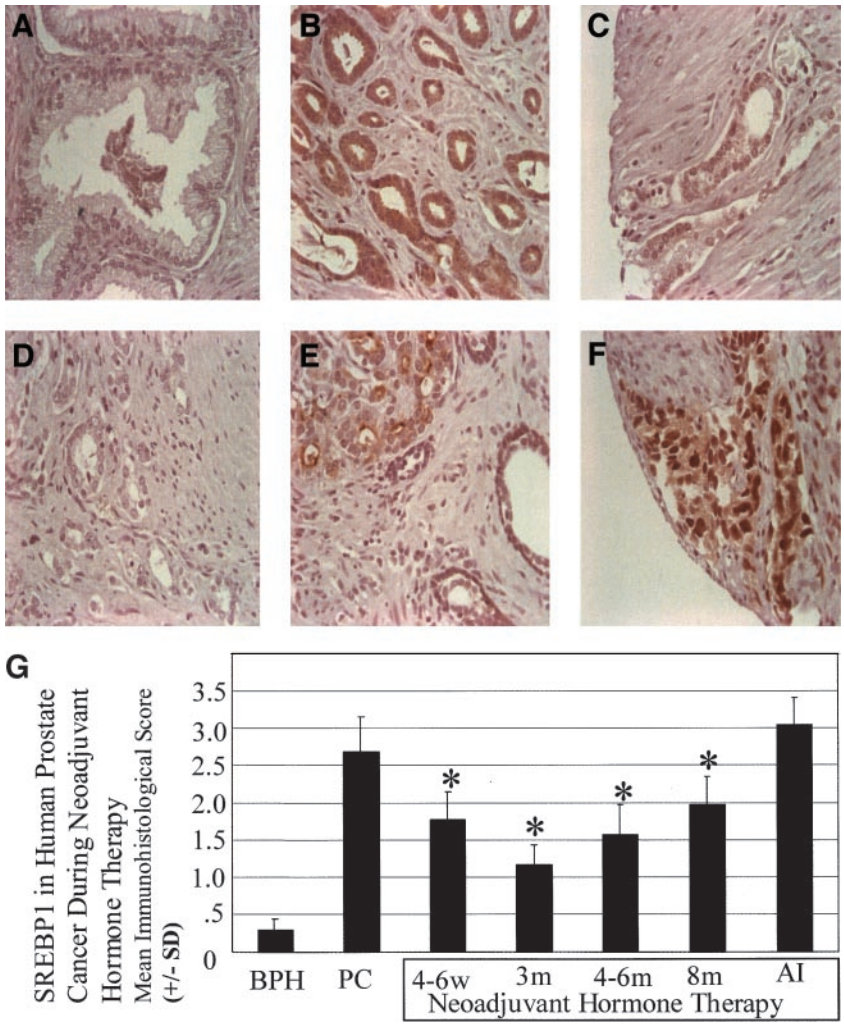

Fig. 7. Sterol response element-binding protein (SREBP)-1 is elevated in clinical prostate samples and androgen regulated. SREBP-1 staining of a representative prostate sample tissue array from patients with benign prostatic hypertrophy (*A*), prostate cancer (*B*), 6–8 weeks of neoadjuvant hormone therapy (*C*), 3 months of neoadjuvant hormonal therapy (*D*), 8 months of neoadjuvant hormonal therapy (*E*), and androgen independence (*F*) is shown. Magnification, ×400. Immunohistological score (*G*; mean ± SE; combination of area and intensity) of 400 human prostate samples from patients with benign prostatic hypertrophy; prostate cancer (*PC*); neoadjuvant hormonal therapy for 4–6 weeks (*4–6w*), 3 months (*3m*), 4–6 months (*4–6m*), or 8 months (*8m*); and androgen independence (*AI*). ∗, statistical significance ($P < 0.05$).

cholesterol synthesis pathway [FDPS (8)]. FAS is a key enzyme involved in *de novo* biosynthesis of fatty acids. Most normal adult tissues express very low levels of FAS and, instead, use dietary circulating fatty acids for biosynthesis (46). We report here that FAS mRNA expression in human prostate xenograft tumors decreased for 14 days after castration and then increased as the tumor progressed to androgen independence. In another prostate xenograft tumor (CWR22), castration caused decreases in FAS protein expression, which increased again when androgen was administered 21–28 days after castration (47). Additionally, others have reported that in LNCaP cells, androgens stimulated the expression of FAS as well as other lipogenic genes (8, 48). In human ovarian, endometrial, breast, and prostate cancers, overexpression of FAS was correlated with advanced pathological stage (49). Furthermore, the role of FAS in cancer cells was critical to their survival because it was demonstrated that administration of an inhibitor of FAS, cerulenin, induced apoptosis of an AI human prostate carcinoma cell line (50). *In vivo*, a 4-fold reduction of tumor growth in an AI human prostate cancer xenograft after treatment with the FAS inhibitor c75 (51) was reported. Interestingly, cell lines that overexpressed FAS were more sensitive to cerulenin than cells that did not overexpress FAS, suggesting that cancer cells require endogenous fatty acid biosynthesis because of increased demand (52–55). This increased requirement by cancer cells of fatty acid synthesis may prove to be a target for therapeutics in prostate cancer.

FDPS plays a critical role in cholesterol homeostasis. Interestingly, the FDPS expression profile in the LNCaP tumor progression series paralleled that of SREBP-2, gradually increasing during progression. Increased SREBP-2 and FDPS may help maintain high levels of cholesterol in prostate tumors despite the loss of androgen. Some types of cancer cells lack the feedback regulatory systems for cholesterol and fatty acid uptake (56). In normal human prostate epithelial cells, SREBP-2 transcriptionally regulated expression of LDL receptor (carrier of cholesterol and fatty acids) mRNA, which was feedback-regulated by LDL and cholesterol. However, in human prostate cancer cell lines that are not androgen responsive (PC-3 and DU145), expression of SREBP-2 and LDL receptor was not down-regulated by cholesterol (56). This loss of feedback regulation of SREBP2 and its downstream effector LDL receptor, in advanced cancer cells, may result in increased fatty acid uptake, providing energy and structural lipids for membranes (52).

SCAP contains a sterol-sensing domain and is regulated by sterol levels. SCAP looses its proteolytic activity when sterols reach high levels within the cell (19). Recently, it has been demonstrated *in vitro* in LNCaP cells that androgens induced an increased expression of SCAP, which enhanced the production of cleaved SREBP and stimulated lipogenic gene expression (23). As we have shown in this present work, removal of androgen (castration) caused a decreased RNA expression of SCAP. Interestingly, this decreased expression was eventually reversed as the tumor progressed to an AI phenotype similar to other androgen-regulated genes. The mature forms of SREBPs did not decrease after castration as mentioned above. Cleaved product of SREBP-2 protein was significantly increased during progression, and the cleaved product of SREBP-1a and

-1c remained relatively constant. Therefore, SCAP is not the only factor involved in the regulation of SREBP activity. Caspase 3 is also involved in SREBP cleavage and activation, as has been reported previously (17, 18). We have shown in our LNCaP cell model that caspase 3 mRNA expression is increased after androgen stimulation,[1] and we are currently evaluating our xenograft tumor model for a role of caspase 3.

As we have shown, clinical human prostate tumors have elevated SREBP-1 protein levels compared with normal prostate tissue or benign prostatic hypertrophy tissue. These elevated levels of SREBP-1 in prostate cancer are decreased by treating patients with neoadjuvant hormone therapy, which decreases levels of testosterone. However, when a tumor develops an AI phenotype, SREBP-1 levels are once again elevated.

In conclusion, these experiments provide the first *in vivo* demonstration that castration induces changes in the expression and activities of SREBP-1a, -1c, and SREBP-2 in LNCaP tumors that result in coordinated regulation, during progression to androgen independence, of several genes involved in fatty acid biosynthesis, energy production, cholesterol synthesis and membrane production, and the transport of acyl-CoA and cholesterol, as summarized in Fig. 1. We also show for the first time that human prostate tumors have elevated levels of SREBP-1 compared with benign prostatic hypertrophy tumors and that androgen withdrawal decreases the expression of SREBP-1. Furthermore, we show that when prostate tumors progress to an AI phenotype, SREBP-1 is once again elevated. The dysregulated expression and activity of SREBPs after androgen withdrawal activate pathways critical to survival and may help facilitate progression to androgen independence. These genes and pathways may provide potential targets for therapy directed against AI prostate carcinoma.

ACKNOWLEDGMENTS

We thank John Cavanagh, Mary Bowden, and Howard Tearle for excellent technical assistance.

REFERENCES

1. Feldman BJ, Feldman D. The development of androgen-independent prostate cancer. Nat Rev Cancer 2001;1:34–45.
2. Gleave ME, Hsieh JT, Gao CA, von Eschenbach AC, Chung LWK. Acceleration of human prostate cancer growth in vivo by factors produced by prostate and bone fibroblasts. Cancer Res 1991;51:3753–61.
3. Gleave ME, Hsieh JT, von Eschenbach AC, Chung LWK. Prostate and bone fibroblasts induce human prostate cancer growth in vivo: implications for bidirectional stromal-epithelial interaction in prostate cancer growth and metastasis. J Urol 1992; 147:1151–9.
4. Gleave ME, Hsieh JT, Wu HC, von Eschenbach AC, Chung LWK. Serum prostate-specific antigen levels in mice bearing human prostate LNCaP tumors are determined by tumor volume and endocrine and growth factors. Cancer Res 1992;52:1598–605.
5. Hsieh JT, Wu, H-C, Gleave ME, von Eschenbach AC, Chung LWK. Autocrine regulation of PSA gene expression in a human prostatic cancer (LNCaP) subline. Cancer Res 1993;53:2852–7.
6. Wu H-C, Hsieh JT, Gleave ME, Chung LWK. Derivation of androgen-independent human LNCaP prostate cancer cell lines: role of bone stromal cells. Int J Cancer 1994;57:406–12.
7. Gleave ME, Tolcher A, Miyake H, Beraldi E, Goldie J. Progression to androgen-independence is delayed by antisense Bcl-2 oligodeoxynucleotides after castration in the LNCaP prostate tumor model. Clin Cancer Res 1999;5:2891–8.
8. Swinnen JV, Ulrix W, Heyns W, Verhoeven G. Coordinate regulation of lipogenic gene expression by androgens: evidence for a cascade mechanism involving sterol regulatory element binding proteins. Proc Natl Acad Sci USA 1997;94:12975–80.
9. Yokoyama C, Wang X, Briggs MR, et al. SREBP-1, a basic helix-loop-helix leucine zipper protein that controls transcription of the LDL receptor gene. Cell 1993;75: 187–97.
10. Hua X, Yokoyama C, Wu J, et al. SREBP-2, a second basic-helix-loop-helix-leucine zipper protein that stimulates transcription by binding to a sterol regulatory element. Proc Natl Acad Sci USA 1993;90:11603–7.
11. Brown MS, Goldstein JL. The SREBP pathway: regulation of cholesterol metabolism by proteolysis of a membrane-bound transcription factor. Cell 1997;89:331–40.
12. Hua X, Sakai J, Ho YK, Goldstein JL, Brown MS. Hairpin orientation of sterol regulatory element binding protein-2 in cell membranes as determined by protease protection. J Biol Chem 1995;270:29422–7.
13. Duncan EA, Brown MS, Goldstein JL, Sakai J. Cleavage site for sterol-regulated protease localized to a Leu-Ser bond in lumenal loop of sterol regulatory element binding protein-2. J Biol Chem 1997;272:12778–85.
14. Sakai J, Nohturfft A, Goldstein JL, Brown MS. Cleavage of sterol regulatory element-binding proteins (SREBPS) at site-1 requires interaction with SREBP cleavage-activating protein. Evidence from in vivo competition studies. J Biol Chem 1998;273:5785–93.
15. DeBose-Boyd RA, Brown MS, Li WP, et al. Transport-dependent proteolysis of SREBP: relocation of site-1 protease from Golgi to ER obviates the need for SREBP transport to Golgi. Cell 1999;99:703–12.
16. Sakai J, Duncan EA, Rawson RB, et al. Sterol-regulated release of SREBP-2 from cell membranes requires two sequential cleavages, one within a transmembrane segment. Cell 1996;85:1037–46.
17. Pai J-T, Brown MS, Goldstein JL. Purification and cDNA cloning of a second apoptosis-related cysteine protease that cleaves and activates sterol regulatory element binding proteins. Proc Natl Acad Sci USA 1996;93:5437–42.
18. Wang X, Zelenski NG, Yang J, et al. Cleavage of sterol regulatory element binding proteins (SREBPs) by CPP32 during apoptosis. EMBO J 1996;15:1012–20.
19. Brown MS, Goldstein JL. Cleavage of sterol regulatory element-binding proteins (SREBPs) at a site-1 requires interaction with SREBP cleavage-activating protein. Evidence from in vivo competition studies. Proc Natl Acad Sci USA 1999;96: 11041–8.
20. Wang X, Sato R, Brown MS, Hua X, Goldstein, LL. SREBP-1, a membrane bound transcription factor released by sterol-regulated proteolysis. Cell 1994;77:53–62.
21. Swinnen JV, Verhoeven G. Androgens and the control of lipid metabolism in human prostate cancer cells. J Steroid Biochem Mol Biol 1998;65:191–8.
22. Miyake H, Nelson C, Rennie P, Gleave ME. Overexpression of insulin-like growth factor binding protein-5 helps accelerate progression to androgen-independence in the human prostate LNCaP tumor model through activation of phosphatidylinositol-3-kinase pathway. Endocrinology 2000;141:2257–65.
23. Heemers H, Maes B, Foufelle F, et al. Androgens stimulated lipogenic gene expression in prostate cancer cells by activation of the sterol regulatory element-binding protein cleavage activating protein/sterol regulatory element-binding protein pathway. Mol Endocrinol 2001;15:1817–28.
24. Swinnen JV, Alen P, Heyns W, Verhoeven G. Identification of diazepam-binding inhibitor/acyl-CoA-binding protein as a sterol regulatory element-binding protein-responsive gene. J Biol Chem 1998;273:19938–44.
25. Swinnen JV, Esquenet M, Heyns W, Rombauts W, Verhoeven G. Androgen regulation of the messenger RNA encoding diazepam-binding inhibitor/acyl-CoA-binding protein in the human prostatic adenocarcinoma cell line LNCaP. Mol Cell Endocrinol 1994;104:153–62.
26. Swinnen JV, Vercaeren I, Esquenet M, Heyns W, Verhoeven G. Androgen regulation of the messenger RNA encoding diazepam-binding inhibitor/acyl-CoA-binding protein in the rat. Mol Cell Endocrinol 1996;118:65–70.
27. Swinnen JV, Van Veldhoven PP, Esquenet M, Heyns W, Verhoeven G. Androgens markedly stimulate the accumulation of neutral lipids in the human prostatic adenocarcinoma cell line LNCaP. Endocrinology 1996;137:4468–74.
28. Horton JD, Shimomuraa I. Sterol regulatory element-binding proteins: activators of cholesterol and fatty acid biosynthesis. Curr Opin Lipidol 1999;10:143–50.
29. Roth G, Kotzka J, Kremer L, et al. MAP kinases Erk1/2 phoshorylate sterol regulatory element-binding protein (SREBP)-1a at serine 117 in vitro. J Biol Chem 2000;275: 33302–7.
30. Xiong S, Chirala SS, Wakil SJ. Sterol regulation of human fatty acid synthase promoter I requires nuclear factor-Y- and Sp-1-binding sites. Proc Natl Acad Sci USA 2000;97:3948–53.
31. Shea-Eaton W, Lopez D, McLean MP. Yin yang 1 protein negatively regulates high-density lipoprotein receptor gene transcription by disrupting binding to sterol regulatory element binding protein to the sterol regulatory element. Endocrinology 2001;142:49–58.
32. Sundqvist A, Ericsson J. Transcription-dependent degradation controls the stability of the SREBP family of transcription factors. Proc Natl Acad Sci USA 2003;100: 13833–8.
33. Yabe D, Brown MS, Goldstein JL. Insig-2, a second endoplasmic reticulum protein that binds SCAP and blocks export of sterol regulatory element-binding protein. Proc Natl Acad Sci USA 2002;99:12753–8.
34. Sheng Z, Otani H, Brown MS, Goldstein LL. Independent regulation of sterol regulatory element binding proteins 1 and 2 in hamster liver. Proc Natl Acad Sci USA 1995;92:935–8.
35. Rasmussen JT, Rosendal J, Knudsen J. Interaction of acyl-CoA binding protein (ABCP) on processes for which acyl-CoA is a substrate, product or inhibitor. Biochem J 1993;292:907–13.
36. Rasmussen JT, Faergeman NJ, Kristiansen K, Knudsen J. Acyl-CoA-binding protein (ACBP) can mediate intermembrane acyl-CoA transport and donate acyl-CoA for β-oxidation and glycerolipid synthesis. Biochem J 1994;299:165–70.
37. Mandrup S, Jepsen R, Skott H, et al. Effect of heterologous expression of acyl-CoA-binding protein on acyl-CoA level and composition in yeast. Biochem J 1993;290: 369–74.
38. Papadopoulos V, Brown AS. Role of the peripheral-type benzodiazepine receptor and the polypeptide diazepam binding inhibitor in steroidogenesis. J Steroid Biochem Mol Biol 1995;53:103–10.
39. Papadopoulos V, Amri H, Boujrad N, et al. Peripheral benzodiazepine receptor in cholesterol transport and steroidogenesis. Steroids 1997;62:21–8.

[1] Unpublished observations.

40. Papadopoulos V, Amri H, Li H, et al. Targeted disruption of the peripheral-type benzodiazepine receptor gene inhibits steroidogenesis in the R2C Leydig tumor cell line. J Biol Chem 1997;272:32129–35.
41. Bono F, Lamarch I, Prabonnaud V, Le Fur G, Herbert JM. Peripheral benzodiazepine receptor agonists exhibit potent antiapoptotic activities. Biochem Biophys Res Commun 1999;265:457–61.
42. Stoebner PE, Carayon P, Casellas P, et al. Transient protection by peripheral benzodiazepine receptors during the early events of ultraviolet light-induced apoptosis. Cell Death Differ 2001;8:747–53.
43. Papadopoulos V, Dharmarajan MM, Li H, et al. Mitochondrial peripheral-type benzodiazepine receptor expression Correlation with gonadotropin-releasing hormone (GnRH) agonist-induced apoptosis in the corpus luteum Biochem Pharmacol 1999;58:1389–93.
44. Hardwick M, Fertikh D, Culty M, et al. Peripheral-type benzodiazepine receptor (PBR) in human breast cancer: correlation of breast cancer cell aggressive phenotype with PBR expression, nuclear localization, and PBR-mediated cell proliferation and nuclear transport of cholesterol. Cancer Res 1999;59:831–42.
45. Petrescu AD, Paynes HR, Boedecker A, et al. Physical and functional interaction of acyl-CoA-binding protein with hepatocyte nuclear factor-4α. J Biol Chem 2003;278:51813–24.
46. Weiss L, Hoffmann GE, Schreiber R, et al. Fatty-acid biosynthesis in man: a pathway of minor importance. Purification, optimal assay conditions, and organ distribution of fatty-acid synthase. Biol Chem Hoppe-Seyler 1986;367:905–12.
47. Myers RB, Oelschlager DK, Weiss HL, Frost AR, Grizzle WE. Fatty acid synthase: an early molecular marker of progression of prostatic adenocarcinoma to androgen-independence. J Urol 2001;165:1027–32.
48. Swinnen JV, Esquenet M, Goossens K, Heyns W, Verhoeven G. Androgens stimulate fatty acid synthase in human prostate cancer cell line LNCaP. Cancer Res 1997;57:1086–90.
49. Epstein JI, Carmichael M, Partin AW. OA-519 (fatty acid synthase) as an independent predictor of pathologic stage in adenocarcinoma of the prostate. Urology 1995;45:81–6.
50. Furuya Y, Akimoto S, Yasuda K, Ito H. Apoptosis of androgen-independent prostate cell line induced by inhibition of fatty acid synthesis. Anticancer Res 1997;17:4589–94.
51. Pizer ES, Pflug BR, Bova GS, et al. Increased fatty acid synthase as a therapeutic target in androgen independent prostate cancer progression. Prostate 2001;47:102–10.
52. Pizer ES, Wood FD, Pasternack GR, Kuhajda FP. Fatty acid synthase (FAS): a target for cytotoxic antimetabolites in HL-60 promyelocytic leukemia cells. Cancer Res 1996;56:745–51.
53. Pizer ES, Chrest FJ, DiGiuseppe JA, Han WF. Pharmacological inhibitors of mammalian fatty acid synthase suppress DNA replication and induce apoptosis in tumor cell lines. Cancer Res 1998;58:4611–5.
54. Pizer ES, Thupari J, Han WF, et al. Malonyl-coenzyme-A is a potential mediator of cytotoxicity induced by fatty-acid synthase inhibition in human breast cancer cells and xenografts. Cancer Res 2000;60:213–8.
55. Kuhajda FP, Pizer ES, Li JN, et al. Synthesis and antitumor activity of an inhibitor of fatty acid synthase. Proc Natl Acad Sci USA 2000;97:3450–4.
56. Chen Y, Hughes-Fulford M. Human prostate cancer cells lack feedback regulation of low-density lipoprotein receptor and its regulator SREBP2. Int J Cancer 2001;91:41–5.